Estuarine, Coastal and Shelf Science (2002) **54,** 89–100
doi:10.1006/ecss.2001.0830, available online at http://www.idealibrary.com on IDEAL®

On the Dispersion and Diffusion Near Estuaries and Around Islands

R.-S. Tseng[a]

Department of Marine Resources, National Sun Yat-sen University, Kaohsiung, Taiwan 804

Received 5 September 2000 and accepted in revised form 13 February 2001

A series of diffusion experiments using surface drifters were performed in the coastal waters of south-western Taiwan near a small estuary and around an island. Two stages or regimes of drifter dispersion can be identified for all experiments: a coherent regime in the beginning stage when the drifters remained clustered with little dispersion occurred, and a rapid-disperse regime in the latter stage when the separation of drifters grew to the order of a few kilometres. Our results show that near estuaries the extent of the dispersive influence is limited to the tidal excursion distance, and the dispersion coefficient is about $12 \sim 15\ m^2\ s^{-1}$. On the other hand, the dispersion coefficient downstream of an island in a strong flow ($\sim 1{\cdot}5\ m\ s^{-1}$) can reach a much larger value ($45\ m^2\ s^{-1}$), which can be attributed to the enhanced mixing and transport processes due to island wakes. Theoretical scaling parameters for coastal water flows are also presented to predict the formation of island wakes. After applying three different methods to exclude the effects of shear flow, the turbulent diffusivities for our experiments amount to $0{\cdot}2 \sim 5\ m^2\ s^{-1}$. Analysis of the differential kinematic properties indicates that a close relationship exists among the dispersion, diffusion and the effect of shear flow.

Keywords: dispersion; diffusion; island wakes; estuary; drifter

Introduction

The pollution of the coastal environment by the discharge of various contaminants into the ocean and its impact on the marine ecosystem has become an ever-growing problem throughout the world. In order to predict accurately dispersion phenomena in coastal seas, estuaries and bays, it is necessary to estimate the horizontal eddy diffusivity and dispersion coefficient. Yanagi (1999) summarized a number of methods for estimating the magnitude of the horizontal diffusion coefficient. These methods can be categorized into the so-called Eulerian or Lagrangian descriptions of fluid flows. In the Eulerian method an array of fixed-location recording current meters are deployed at the ocean site and the dispersion rate can be deduced from the observed scales of motion (Winant, 1983). On the other hand, information about the Lagrangian descriptions of flows and dispersion behaviour can be collected by tracking groups of drifting floats (Yanagi *et al.*, 1982; Pal & Sanderson, 1992) or dye-patch growth (Elliott *et al.*, 1997; Riddle & Lewis, 2000). Note that in the Lagrangian case, it is the apparent horizontal diffusivity which is estimated directly from the rate of change of the variance of dye concentration or float dispersion, and the effect of shear flow has to be excluded in order to obtain the true turbulent diffusivity (Yanagi, 1999).

The role of tidal dispersion was reassessed and quantified by Geyer and Signell (1992) based on a consideration of the relevant physical mechanisms and results from numerical simulations. One of their main conclusions is that tidal dispersion is likely to be a dominant agent for horizontal mixing in regions of abrupt topographic variance such as headlands and inlets. Geyer and Signell (1992) also point out that the principal influence of tidal currents on dispersion occurs at length scales of the tidal excursion and smaller. More recently, Inoue and Wiseman (2000) investigated the transport and mixing processes in a Louisiana estuary using numerical modelling. Their results suggest that coastal trapping, that includes not only trapping by shoreline irregularities but also trapping by islands, could significantly enhance particle dispersion. Furthermore, in estuarine and coastal environments the varying influence of density-driven and wind-driven currents may obscure the contribution of tidal dispersion. Therefore, to better our understanding of transport, stirring and mixing processes in such a complicated system, more observations are needed to quantify each individual influence such as bottom and coastal topography as well as the strength and character of the tidal currents. In this contribution results from three separate float

[a]Corresponding author. E-mail: rstseng@mail.nsysu.edu.tw

0272–7714/02/010089+12 $35.00/0

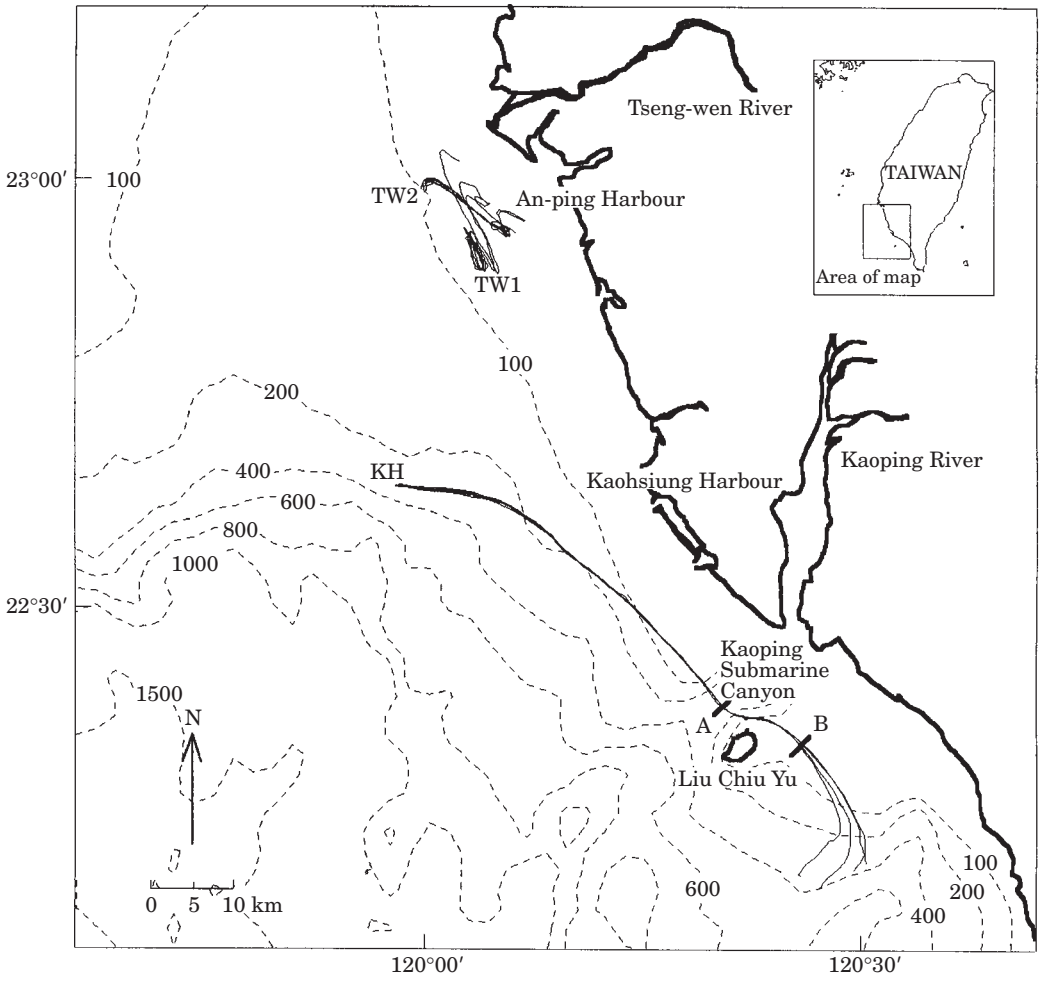

FIGURE 1. The location of deployment and overall trajectories of drifter experiments TW1, TW2 and KH. The insert is a large-scaled map of Taiwan. The positions of A and B in the KH trajectories correspond to those of Figure 2.

dispersion experiments conducted on the southwestern Taiwan shelf in 1996 are presented. The dispersivities and diffusivities for two different experimental conditions encountered in this study, i.e., in a small estuarine zone and around an island, are discussed and compared with each other.

Experiments

Three experiments of drifter cluster dispersion were carried out in the coastal waters of southwestern Taiwan in the vicinity of Tseng-wen estuary and Kaohsiung Harbour (Figure 1). These areas are sites for several pollutant-releasing activities such as the dumping of coal ashes from a steel plant, the discharge of thermal effluent from a power plant, and the offshore sand-mining for constructional use. Therefore, a better understanding of the diffusive properties and flow characteristics in these areas is essential to the ecology, chemistry, and water quality management. Two experiments, designated as TW1 and TW2, were conducted in January and April of 1996 at the Tseng-wen estuarine zone approximately 6–10 km away from the river mouth over $10 \sim 80$ m water depths. This area has a smooth and gently sloping bathymetry, leading to water 60 m deep at about 10 km from shore. The coastline is orientated NW/SE, forming a semi-embayment near the estuary and has little geomorphic complexity. Tides in this area are mixed, with semi-diurnal tides dominating. Major tidal constituents are M_2, S_2, O_1 and K_1. The third experiment, designated as KH, was conducted farther offshore in the vicinity of Kaohsiung Harbour and Kaoping Submarine Canyon in February 1996. This site is characterized by a rapidly changing bottom topography with water depth varying from about 1000 m to less than 100 m, especially in the Kaoping Submarine Canyon. One principal feature of interest

TABLE 1. Information about each drifter experiment

Experiment designation	Cluster deployment		Number of driftrs	Experiment duration (h)	Place of deployment and its water depth
	Time (h)	Date			
TW1	1300	4 January 1996	4	23	Tseng-wen (− 60 m)
TW2	1250	23 April 1996	5	18	Tseng-wen (− 80 m)
KH	1240	15 February 1996	4	26	Kaohsiung (− 200 m)

in this study is the island of Liu-Chiu-Yu, which is about 14 km offshore from the Kaoping River mouth. The area of this island is 6·8 km^2 and the length of the long axis is about 5·5 km. Winds over the southwestern Taiwan coast are dominated by the NE monsoon with mean speeds up to 8–10 m s^{-1} from late September to early April. From June to August, the prevailing winds are southwesterly with mean speeds less than 8 m s^{-1}. Tides and tidal currents in the Kaohsiung areas are of the mixed type according to previous observations. Furthermore, coastal currents in this area are also affected by the Kuroshio and its branches.

In each experiment four or five surface drifters were tracked simultaneously. This is a minimum requirement ($n \geqq 4$) for the number of drogues to determine the velocity gradients, centroid speeds and turbulence velocities using the linear regression procedures with sufficient statistics (Okubo & Ebbesmeyer, 1976). The surface drifter (Clearwater Inc., Watertown, MA, U.S.A.) is of the CODE type (Davis, 1985) with GPS/ARGOS position fixing system. Drag producing vanes are made of plasticized cloth (100 cm × 50 cm) which are situated just beneath the water surface when deployed. Four floats are added for adequate buoyancy. The drifters were designed to be accurate surface current followers in the presence of wind and surface waves. Drifter locations are fixed using a GPS and the data were transmitted back via the ARGOS system. Typically, estimated error of the GPS/ARGOS fixings of this system is of the order of 60 m. The drifters were deployed on the corners of a 100-m square or pentagon. Drifters were tracked for 18–26 h with positions fixed every 20–30 min. The drifters had xenon flash with ropes attached to aid in recovery after the experiments were completed. Table 1 lists the number of drifters, the time and location of release and the duration for each experiment.

Because the times of fixing for all the drifters in each experiment were not synchronized, it was necessary to interpolate the position of the drifters at given fixed intervals during the studies. A cubic spline method was applied to each original drifter trajectory, and new positions were interpolated at 20 min intervals. The drogue speeds were inferred from the splined trajectories with centered difference except for the first and last points where forward and backward differences were applied, respectively. The error of the flow speeds inferred from the drifter tracks is thus estimated to be approximately 60 m/20 min = 5 cm s^{-1}.

Results and discussion

Mean flow pattern

Plotted in Figure 1 are the location map and overall trajectories for all drifter experiments in this study. It is clear that for the experiments TW1 and TW2, which were both conducted at the same location (Tseng-wen estuary), the drifter tracks mainly display tidal excursion characteristics with a distance about 10 km. A high degree of spatial coherency can be seen for the drifter tracks in both experiments. The centroid velocities calculated from the regression method of Okubo and Ebbesmeyer (1976) in the alongshore and shoreward directions (u and v) are plotted as a function of time in Figures 2(a), (b) and (c) respectively for each experiment. The predicted times of high and low waters at the nearby An-Ping Harbour just south of the Tseng-wen river-mouth are also plotted in Figures 2(a) and (c) to compare with the drifter trajectories and velocities. It is found that the drifters were moving mainly in the alongshore direction, and the longshore velocities showed strong semi-diurnal tidal variations. The drifters generally moved northward during flooding stage, and moved southward during ebbing stage. The amplitude of tidal speeds is around $50 \sim 60$ cm s^{-1}. Previous studies of fixed-location current measurements taken with a SeaPac 2100 held by a tripod deployed off the Tseng-wen river-mouth at an average water depth of 3·8 m was reported by Liu *et al.* (1999). Their results indicate that the observed currents are essentially alongshore at predominantly semi-diurnal frequencies, having a slightly onshore tendency during the flood (northward tidal current) and offshore tendency during the ebb. Their results are consistent with our drifter trajectories and velocities obtained from the experiments TW1 and TW2.

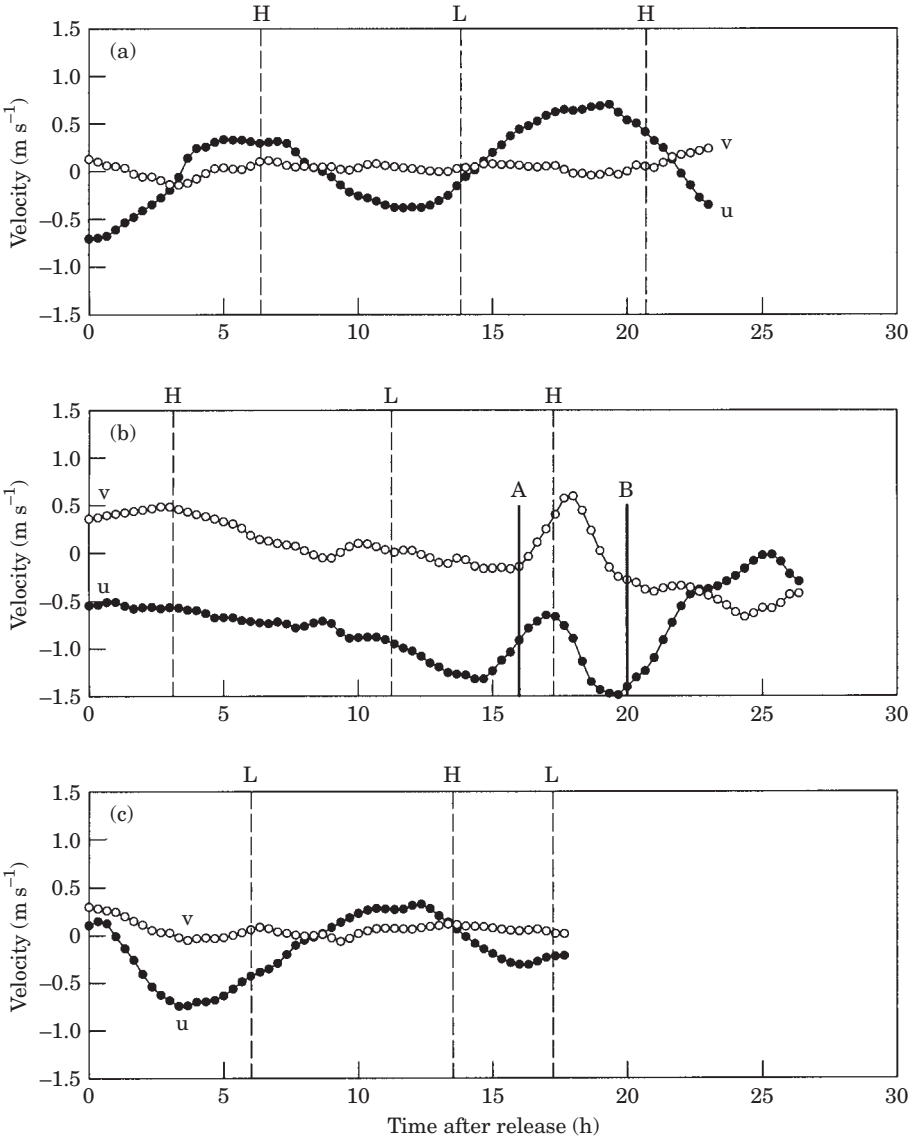

FIGURE 2. Centroid velocity as a function of time for the experiments of (a) TW1, (b) KH and (c) TW2. The label u (solid circle) indicates the alongshore velocity component (positive towards the northwest) and v (open circle) the shoreward velocity component. Dotted lines indicate the predicted times of high and low waters in the nearby harbour. Two solid lines marked by A and B in Figure 2(b) are plotted to indicate the time of arrival and departure, respectively, near island (see the locations of A and B in Figure 1).

Now we turn our attention to the experiment KH. In a similar time span of about 24 h, drifters of the experiment KH travelled a much longer distance ($\sim$80 km) than those of the experiments TW1 and TW2 (Figure 1), indicating a swift flow was present at the times of the former experiment. Note that in this experiment four drifters were deployed at a location approximately 40 km west of Kaohsiung Harbour with water depth over 200 m. The drifters headed eastward during the first 6 h at a speed of about 0·6 m s^{-1}, and then accelerated to a high speed of 1·4 m s^{-1} in the downcoast direction confronting the island of Liu-Chiu-Yu [Figure 2(b)]. Due to the interruption of such obstructions to the flows, the drifters decelerated and made a detour around the island. After passing the island, the drifters accelerated again to 1·6 m s^{-1} and then rapidly dispersed at the end of the study period. Unlike the results of the Tseng-wen estuary, drifter velocities at this site appeared to be unaffected by the tides. The predicted times of high and low waters at the nearby Kaohsiung Harbour are also plotted in Figure 2(b) for comparison.

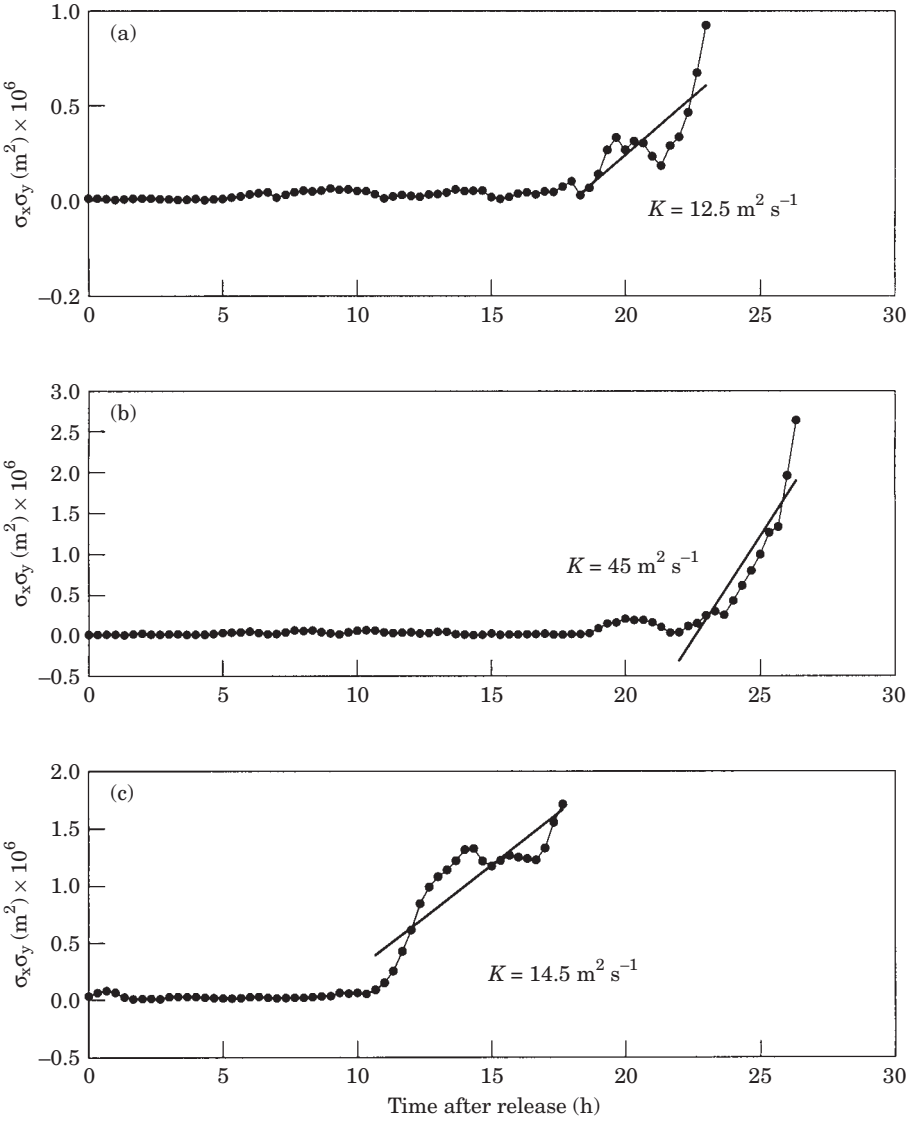

FIGURE 3. Variance (solid circle) $\sigma_x\sigma_y$, of drifter positions *vs* time for the experiments of (a) TW1, (b) KH and (c) TW2. Solid line is a least square fit for the latter stage of each experiment. The values of K are calculated from the slope of the fitted line (see discussion in Section 3.2).

Dispersion and island trapping

For each cluster of drifters, the variances σ_x^2 and σ_y^2 about the centroid along the major and minor axes of the cluster ellipse can be computed, and the geometrically averaged variance is calculated by $\sigma_x\sigma_y$. Figures 3(a), (b) and (c) show the time evolution of $\sigma_x\sigma_y$ of the drifters for the experiments of TW1, KH and TW2. During the first 18 h of the experiment TW1, the size of the drifter cluster, measured by $\sigma_x\sigma_y$, basically remained small and showed a relatively small increase. The size of the cluster increased dramatically during the next 5 h. For the experiment KH, the variance $\sigma_x\sigma_y$ showed a small increase during the first 23 h, and then increased rapidly thereafter [Figure 3(b)]. Similar results of variations of $\sigma_x\sigma_y$ with respect to time can also be found for the experiment TW2, in which the transition of $\sigma_x\sigma_y$ occurs at the time of about 11 h. Therefore, two stages or regimes can be identified for all three experiments: a coherent regime in the beginning stage when the drifters remained clustered and little dispersion occurred, and a rapid-disperse regime in the latter stage when the separations of drifters grew to the order of a few kilometres. Following Yanagi *et al.* (1982) the 2-D mean dispersion coefficient K is defined by

$$K=\frac{1}{4}\frac{d}{dt}\sigma_x\sigma_y \quad (1)$$

The value of K can be estimated from the average slope of $\sigma_x\sigma_y$ with respect to time by linear regression for the latter stage of each experiment. The slope of the regression line was found to vary somewhat with the number of points used in the regression procedure. The dispersion coefficient, as derived from the least square fit, is $12{\cdot}5 \pm 0{\cdot}5$, 45 ± 5, and $14{\cdot}5 \pm 0{\cdot}5$ m^2 s^{-1} respectively for the experiments of TW1, KH and TW2 (Figure 3). This result indicates that the rate of dispersion for the Tseng-wen estuary in January and April has nearly the same magnitude, while the rate of dispersion for the experiment KH has a much larger value.

The larger value of the dispersion coefficient obtained for the experiment KH appears to be due to the effect of island trapping as was illustrated by the numerical simulations of Inoue and Wiseman (2000). It has been well known that flow pattern in the wake of a circular cylinder depends upon the Reynolds number of the flow (Batchelor, 1970). The Reynolds number in coastal waters is now defined as

$$R_e=\frac{UL}{K_H} \quad (2)$$

where U is the representative velocity scale, L is the length of the island, K_H is the horizontal eddy viscosity. When the Reynolds number is above a limiting value (between 60 and 90), eddies are shed continuously from the cylinder and the so-called Karman vortex street is developed. For geophysical flows in shallow coastal waters around an obstacle (island, for example), similar flow structures have been observed using remote-sensing techniques (Pattiaratchi *et al.*, 1986; Cramp *et al.*, 1991; Ferrier *et al.*, 1996). There are serious uncertainties in the evaluations of K_H, varying from $0{\cdot}5$ m^2 s^{-1} in the vicinity of Rattray Island, Australia to $2{\cdot}2 \times 10^2$ m^2 s^{-1} in the Pacific Ocean (Geyer & Signell, 1992). For very shallow waters of depth H, Pattiaratchi *et al.* (1986) have introduced an ' island wake parameter ', P (defined as below) which could be used to describe the wake

$$P=\frac{UH^2}{K_zL} \quad (3)$$

where K_Z is the vertical eddy viscosity. When the island wake parameter is above a limiting value of unity, the island wake is similar to that formed at high Reynolds number. In this study a constant value of 10^2 and 10^{-1} m^2 s^{-1} is adopted respectively for K_H and K_Z following Pattiaratchi *et al.* (1986). The flow velocity is assumed to be $1{\cdot}5$ m s^{-1} [Figure 2(b)] and the length of the island is 5500 m. The mean water depth obtained from the bathymetric chart is taken to be approximately 60 m. As a result, $R_e=82$ and $P=10$. This is indicative of the formation of eddies and a Karman vortex street behind the Liu-Chiu-Yu Island, which are strongly related to the mixing and stirring processes. Therefore, a larger value of dispersion coefficient observed downstream of this island would be a reasonable outcome [Figure 3(b)].

Eddy diffusion

The dispersion estimate obtained from the drifter positions also includes the effects of shear flow and turbulent diffusion. In order to estimate the true horizontal turbulent diffusivity, the shear-induced spreading, rotation and divergence must be removed from the apparent dispersion. A number of techniques have been proposed for this purpose. These are the methods proposed by (1) Okubo and Ebbesmeyer (1976), (2) List *et al.* (1990) and (3) Yanagi *et al.* (1982). A detailed description of each method can be found in Yanagi (1999), and will not be elaborated here.

Turbulent diffusivities were calculated for each experiment using these three methods for comparison. We denote k as the diffusivity suggested by Okubo and Ebbesmeyer, k' as the diffusivity suggested by List *et al.* and k'' as the diffusivity suggested by Yanagi *et al.* The turbulent diffusivity k is estimated by analogy to a combination of mixing length theory and turbulence theory (Okubo & Ebbesmeyer, 1976)

$$\begin{aligned} k_x&=c\sigma_x\sigma_u \\ k_x&=c\sigma_y\sigma_v \\ k&=(k_x+k_y)/2 \end{aligned} \quad (4)$$

where σ_x and σ_y are the root-mean-squares of the relative displacement; σ_u and σ_v are the root-mean-square values of the turbulent velocity, and c is a proportionality constant taken to be $0{\cdot}1$. Figures 4(a), (b) and (c) show k and its 95% confidence interval *vs* time for the experiments of TW1, KH and TW2, respectively. Note that the uncertainty associated with k is estimated from the propagation of errors of σ_x and σ_y (Bevington, 1969). The diffusivities calculated by the method of Okubo and Ebbesmeyer (1976) display two different regimes with respect to the time or length scales. In the beginning stage or the coherent regime, the values of k for all three experiments are small with the magnitudes of less than 1 m^2 s^{-1}. In

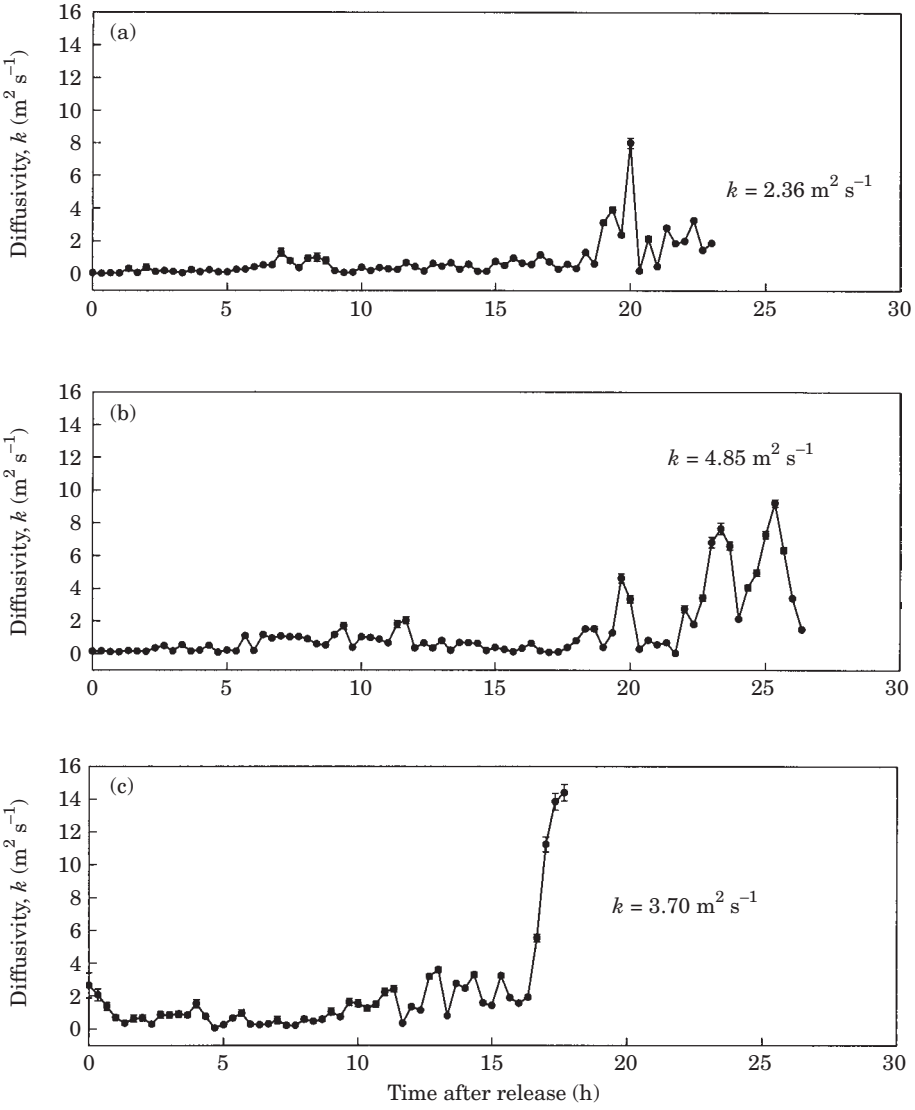

FIGURE 4. Diffusivities obtained using the method of Okubo and Ebbesmeyer (1976) *vs* time for the experiments of (a) TW1, (b) KH and (c) TW2. Bars indicate 95% confidence interval. The values of k are calculated from the mean in the latter stage.

the latter stage or the rapid-disperse regime, the values of k increase rapidly with a mean value of about $2 \sim 5$ m^2 s^{-1}. The trend of variations for k' calculated by the method of List *et al.* (1990) as shown in Figure 5 is similar to that for k, but the values of k' are smaller than those of k. The mean values of k' in the latter stage are approximately $0{\cdot}3 \sim 0{\cdot}9$ m^2 s^{-1}. In the method of Yanagi *et al.* (1982), the ' turbulent ' positions of each drifter due only to the turbulent velocity are evaluated first, and then using the turbulent positions to calculate the variance of k''. Figures 6(a), (b) and (c) show the real geometrically-averaged variance $\sigma_x\sigma_y$, *vs* time for all three experiments. In the beginning stage the variation of $\sigma_x\sigma_y$ *vs* time is more random and irregular. The increase of $\sigma_x\sigma_y$, with time in the latter stage is more marked. The values of k'' were obtained by linear regression of the smoothed time series of $\sigma_x\sigma_y$, with respect to time in the latter stage of each experiment. The obtained values of k'' are approximately $0{\cdot}2 \sim 0{\cdot}6$ m^2 s^{-1} for the three experiments. Therefore the result of k' is more consistent with that of k''. A comparison among results of diffusivity estimated by these three methods indicates that the real horizontal turbulent diffusivity increases as the time and length scales increase, and then it reaches a mean value of around $0{\cdot}2 \sim 5$ m^2 s^{-1} in the latter stage of each experiment. The constant c in the method of Okubo and Ebbesmeyer (1976) as indicated in Equation (4) adds uncertainty to the value of eddy diffusivity. The value of c is proposed to be 0·1

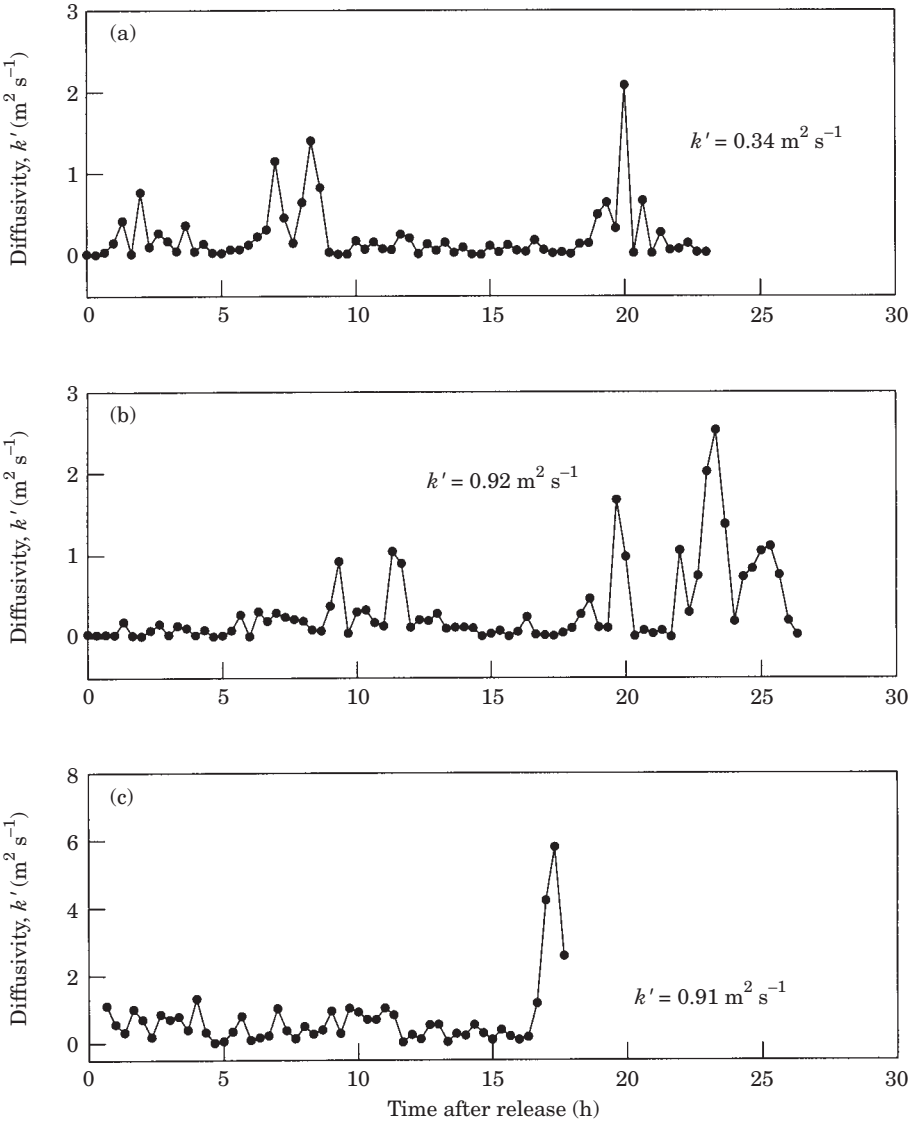

FIGURE 5. Diffusivities obtained using the method of List *et al.* (1990) *vs* time for the experiments of (a) TW1, (b) KH and (c) TW2. The values of k' are calculated from the mean in the latter stage.

or smaller in this study in order to make the results of eddy diffusivity derived from various methods more compatible.

Differential kinematic properties (DKP)

The differential kinematic properties of fluid flow, i.e., divergence, vorticity, shearing deformation rate and stretching deformation rate can be expressed as the following forms

$$\begin{aligned} D &= \partial\overline{u}/\partial x + \partial\overline{v}/\partial y \quad \text{(divergence)} \\ \zeta &= \partial\overline{v}/\partial x - \partial\overline{u}/\partial y \quad \text{(vorticity)} \\ S &= \partial\overline{v}/\partial x + \partial\overline{u}/\partial y \quad \text{(shearing deformation rate)} \\ N &= \partial\overline{u}/\partial x - \partial\overline{v}/\partial y \quad \text{(stretching deformation rate)} \end{aligned} \tag{5}$$

where $\partial\overline{u}/\partial x$, $\partial\overline{u}/\partial y$, $\partial\overline{v}/\partial x$, $\partial\overline{v}/\partial y$ are linear velocity gradients at the centroid. The DKP are important elements in describing the structure of relative motion and for relating the velocity field to dynamical processes. For example, divergence is a measure of vertical motion. Vorticity is indicative of velocity shear and is more related to wind stress and bottom topography. The deformation rates are important in the evolution of oceanic frontal zones.

Okubo and Ebbesmeyer (1976) expanded the velocity field as a Taylor series about the centroid position of a cluster of drifters, and then used linear regression procedures to obtain DKP from trajectories of drifters with a cluster. Plotted in Figures 7(a), (b) and (c) are the horizontal divergence, relative

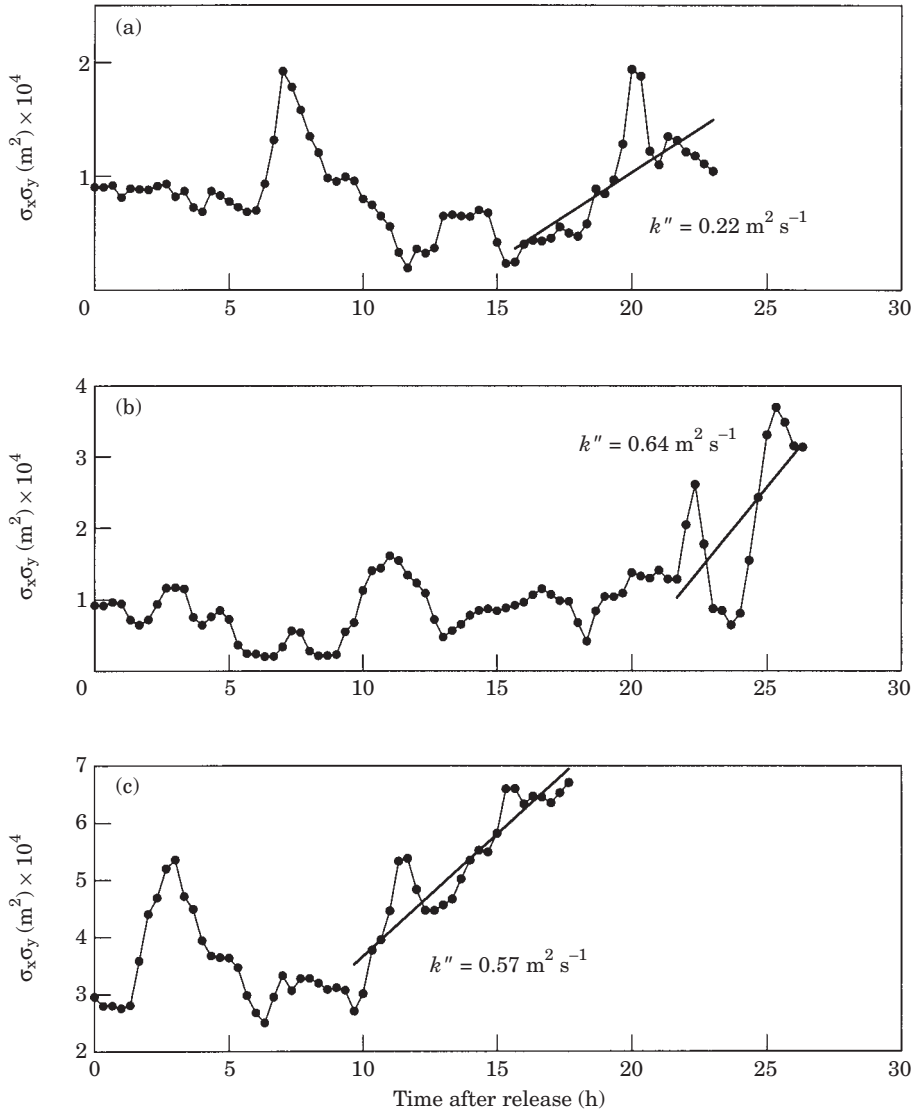

FIGURE 6. Real variance (solid circle), $\sigma_x\sigma_y$, obtained using the method of Yanagi *et al.* (1982) *vs* time for the experiments of (a) TW1, (b) KH and (c) TW2. Solid line is a least square fit for the latter stage of each experiment. The values of k'' are calculated from the slope of the fitted line (see discussion in Section 3.3).

vorticity, stretching and shearing deformation rates and their 95% confidence intervals calculated from the method of Okubo and Ebbesmeyer (1976) for experiments TW1, KH and TW2, respectively. Note that fitting uncertainty of the DKP estimates depends strongly on how many drifters are used in the experiment. Molinari and Kirwan (1975) have demonstrated that the estimates of the DKP from observations of the motions of only three drifters in the western Caribbean Sea displayed ragged character, and the turbulent statistics could not be determined. If more than three drifters are present, the estimates of the DKP should be considerably improved. It is seen from comparison of Figure 7(a) and (c) that calculation of DKP which use five drifters are more smoother and the uncertainties of the DKP are smaller than those which utilize four drifters.

The horizontal divergence for all experiments is characterized by a more frequent sign change in the beginning stage or the coherent regime, afterwards it remains mostly positive. This is consistent with our observations of the increase of variances at later times (Figure 3). The magnitude of fluctuations of the DKP for the experiment KH is larger than that of the experiments TW1 and TW2. This can be attributed to the dramatic difference of bottom topography between these two types of experimental site. The experiments TW1 and TW2 were both conducted at

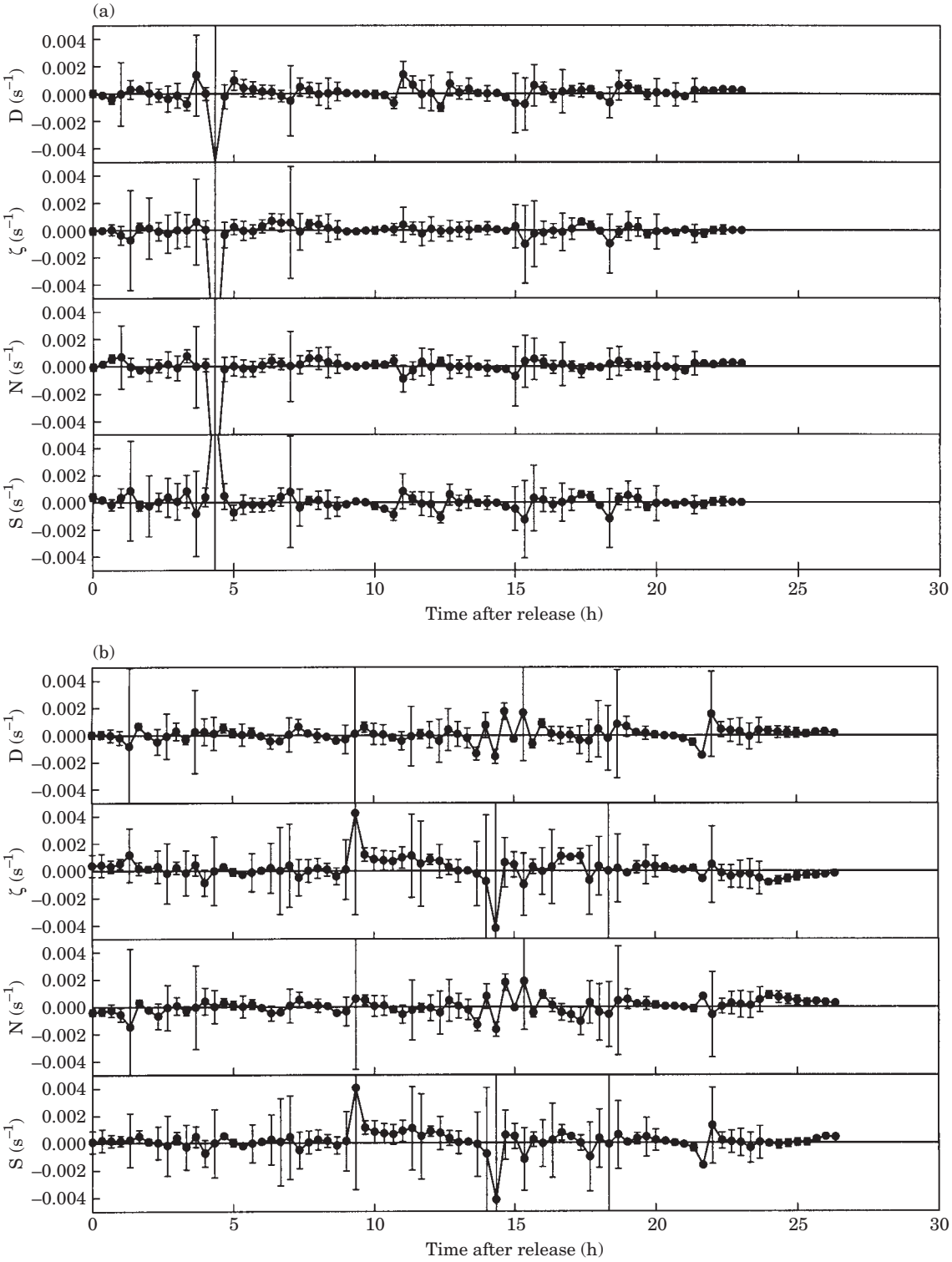

FIGURE 7. (a and b). Divergence (D), vorticity (ζ), stretching deformation rate (N) and shearing deformation rate (S) plotted against time for the experiments of (a) TW1 and (b) KH. Bars indicate 95% confidence interval.

the Tseng-wen estuarine zone in water depth of 10 ~ 80 m, whereas drifter clusters of the experiment KH travelled through abrupt topographic variations in water depth of 50>800 m. Therefore, the values of the DKP were constrained by the ocean depth in the estuarine zone. A prominent example is at the time of

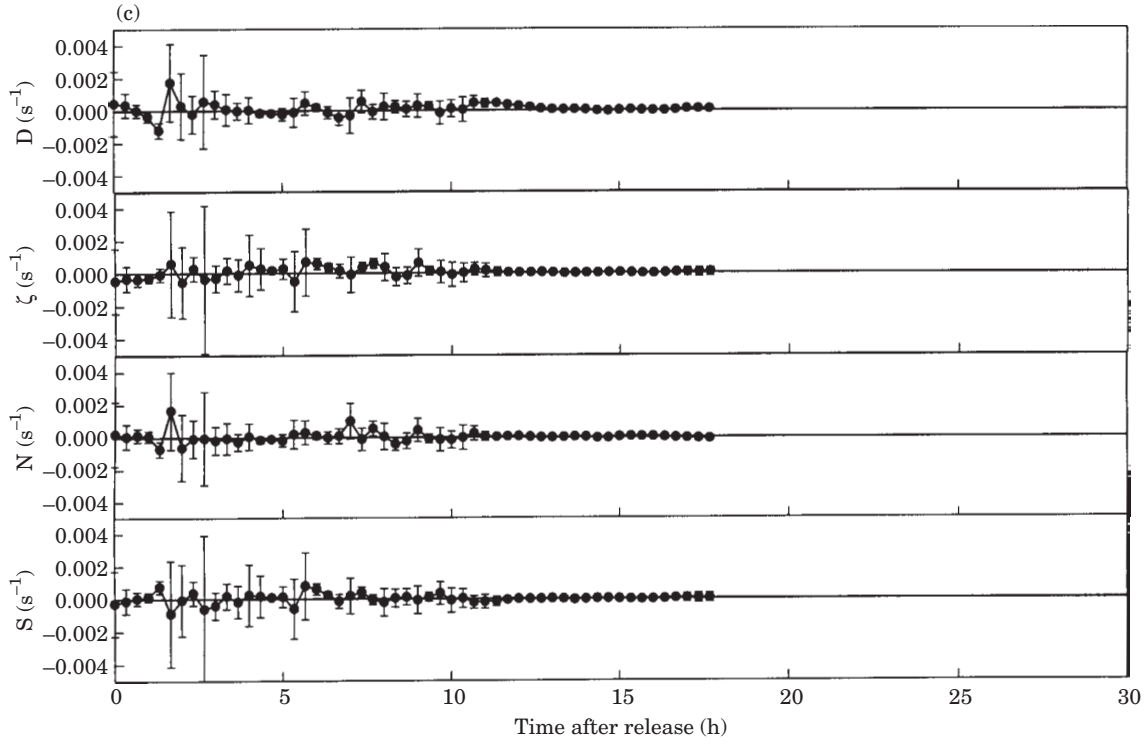

FIGURE 7. (c).

FIGURE 7. Divergence, vorticity, stretching deformation rate and shearing deformation rate plotted against time for the experiments of (a) TW1, (b) KH and (c) TW2. Bars indicate 95% confidence interval.

14 ~ 16 h from release for the experiment KH [Figure 7(b)] when the drifters were crossing the Kaoping Submarine Canyon. Also note that the values of the vorticity and deformation rates in the latter stage of the experiment TW2 are much smaller [Figure 7(c)] than those of the experiment TW1 [Figure 7(a)], indicating that the effect of shear flow is smaller in the former case. Since the apparent dispersion coefficient is about the same magnitude for these two experiments which were conducted in the same estuarine zone (Figure 3), the true turbulent diffusivity obtained by excluding the effect of shear flow will be higher for the experiment TW2. This is in accordance with the results of diffusivity estimates discussed in the previous section (Figures 5 and 6).

Conclusion

The observation and calculations presented here provide quantitative data on the flow pattern, dispersion and diffusion characteristics near a small, tidal-dominant, estuarine zone and around an island, both are located off the south-western Taiwan coast. Two regimes of dispersion in coastal waters can be identified: a coherent regime in the beginning stage and a rapid-disperse regime in the latter stage. Our results show that in the Tseng-wen estuary the main influence of a moderate tidal current is limited to the tidal excursion length, and dispersion coefficients of around $12 \sim 15\ m^2\ s^{-1}$ can be obtained for this case. In another case a strong alongshore current ($\sim 1{\cdot}5\ m\ s^{-1}$) flowing towards the island of Liu-Chiu-Yu produced a high dispersion rate of around $45\ m^2\ s^{-1}$ in the island wakes. This larger value of dispersion coefficient appears to be due to island trapping, the enhanced mixing and transport processes associated with instabilities in the wake and the formation of a vortex street downstream of the island. The scaling parameters computed from the known geometry of island and the measured flow patterns do support this finding.

Turbulent diffusivities computed from the methods of List *et al.* (1990) and Yanagi *et al.* (1982) are roughly of the same magnitude, while the diffusivities computed from Okubo and Ebbesmeyer (1976) are somewhat larger in magnitude assuming the proportionality c is 0·1. However, the trends of variation for k, k' and k'' with respect to time derived from these three methods are remarkably consistent. The diffusivities are negligibly small in the beginning stage, and

increase rapidly in the latter stage, reaching a mean value of $0{\cdot}2 \sim 5\ m^2\ s^{-1}$. It was found that the values of the differential kinematic properties appear to be affected by the bottom topography. The observations reported here also show that the DKP can make a contribution to drifter separation and turbulent diffusivity.

Finally, it should be noted that the effect of the number of drifters on estimates of the DKP and turbulent statistics is profound. As there were only four or five drifters for our experiments, there is insufficient confidence in the estimates of the turbulent statistics. However, as techniques of modern position fixing become considerably inexpensive and sufficiently accurate, the drogue tracking method and the calculations as presented in this paper will be more viable in determining the DKP and diffusivities of the ocean.

Acknowledgements

This work was supported by the National Science Council of the Republic of China under grant number NSC85-2611-P-110-005. The assistance of my former graduate student, Mr Kuo-Rong Hsu, in conducting the field experiments and data analysis is deeply appreciated. I also would like to thank Prof. James T. Liu for reading the manuscript.

References

Batchelor, G. K. 1970 *An Introduction to Fluid Mechanics*. Cambridge University Press, New York, 515 pp.

Bevington, P. R. 1969 *Data Reduction and Error Analysis for the Physical Science*. McGraw-Hill, New York, 336 pp.

Cramp, A., Coulson, M., James, A. & Berry, J. 1991 A note on the observed and predicted flow patterns around islands-Flat Holm, the Bristol Channel. *International Journal of Remote Sensing* **11,** 1111–1118.

Davis, R. E. 1985 Drifter observation of coastal surface currents during CODE: the statistical and dynamical views. *Journal of Physical Oceanography* **90,** 4756–4772.

Elliott, A. J., Barr, A. G. & Kennan, D. 1997 Diffusion in Irish coastal waters. *Estuarine, Coastal and Shelf Science* **44(A),** 15–23.

Ferrier, G., Davies, P. A. & Anderson, J. M. 1996 Remote Sensing observations of a vortex street downstream of an obstacle in an estuarine flow. *International Journal of Remote Sensing* **17,** 1–8.

Geyer, W. R. & Signell, R. P. 1992 A reassessment of the role of tidal dispersion in estuaries and bays. *Estuaries* **15,** 97–108.

Inoue, M. & Wiseman, W. J., Jr. 2000 Transport, mixing and stirring processes in a Louisiana estuary: A model study. *Estuarine Coastal and Shelf Science* **50,** 449–466.

Liu, J. T., Chao, S.-Y. & Hsu, R. T. 1999 The influence of suspended sediments on the plume of a small mountainous river. *Journal of Coastal Research* **15,** 1002–1010.

List, E. J., Gartrell, G. & Winant, C. D. 1990 Diffusion and dispersion in coastal waters. *Journal of Hydraulic Engineering* **116,** 1158–1179.

Molinari, R. & Kirwan, A. D. 1975 Calculations of differential kinematic properties from Lagrangian observations in the western Caribbean Sea. *Journal of Physical Oceanography* **5,** 483–491.

Okubo, A. & Ebbesmeyer, C. C. 1976 Determination of vorticity, divergence, and deformation rates from analysis of drogue observations. *Deep-Sea Research* **23,** 349–352.

Pal, B. K. & Sanderson, B. G. 1992 Measurements of drifter cluster dispersion. *Atmosphere-Ocean* **30,** 621–651.

Pattiaratchi, C., James, A. & Collins, M. 1986 Island wakes and headland eddies: A comparison between remotely sensed data and laboratory experiments. *Journal of Geophysical Research* **92,** 783–794.

Riddle, A. M. & Lewis, R. E. 2000 Dispersion experiments in U.K. coastal water. *Estuarine, Coastal and Shelf Science* **51,** 243–254.

Winant, C. D. 1983 Longshore coherence of currents on the southern California shelf during the summer. *Journal of Physical Oceanography* **13,** 54–64.

Yanagi, T., Murashita, K. & Higuchi, H. 1982 Horizontal turbulent diffusivity in the sea. *Deep-Sea Research* **29,** 217–226.

Yanagi, T. 1999 *Coastal Oceanography*. Terra Scientific Publishing Company, Tokyo, 161 pp.